processes

MDPI

Article

Photolysis, Photocatalysis, and Sorption of Caffeine in Aqueous Media in the Presence of Chitosan Membrane and Chitosan/TiO_2 Composite Membrane

Juliana Prando [1], Ingrid Luíza Reinehr [2], Luiz Jardel Visioli [1], Alexandre Tadeu Paulino [1,3,*] and Heveline Enzweiler [1,2]

[1] Department of Food and Chemical Engineering, Santa Catarina State University, BR 282, km 574, Linha Santa Terezinha, Pinhalzinho 89870-000, SC, Brazil
[2] Postgraduate Program in Food Science and Technology, Santa Catarina State University, BR 282, km 574, Pinhalzinho 89870-000, SC, Brazil
[3] Department of Chemistry, Santa Catarina State University, Rua Paulo Malschitzki, 200, Zona Industrial Norte, Joinville 89219-710, SC, Brazil
* Correspondence: alexandre.paulino@udesc.br

Abstract

Sorption and advanced oxidative processes (AOPs) are potential strategies for the removal of organic compounds, such as caffeine, from aqueous media. Such strategies tend to be more promising when combined with biopolymeric membranes as sorbents and photocatalyst supports. Therefore, the aim of the present study was to investigate sorption and AOP parameters in the performance of chitosan membranes and chitosan/TiO_2 composite membranes in individual and hybrid systems involving the photolysis, photocatalysis, and sorption of caffeine. Caffeine degradation by photolysis was 19.51 ± 1.14, 28.61 ± 0.05, and 30.64 ± 6.32%, whereas caffeine degradation by photocatalysis with catalytic membrane was 18.33 ± 2.20, 20.83 ± 1.49, and 31.41 ± 3.08% at pH 6, 7, and 8, respectively. In contrast, photocatalysis with the dispersed catalyst achieved degradation of 93.56 ± 2.12, 36.42 ± 2.59, and 31.41 ± 1.07% at pH 6, 7, and 8, respectively. These results indicate that ions present in the buffer solutions affect the net electrical charge on the surface of the composite biomaterial with the change in pH variation, occupying active sorption sites in the structure of the biomaterial, which was characterized by Fourier transform infrared spectrometry, thermogravimetric analysis, differential scanning thermogravimetry, and X-ray diffraction. Thus, it is verified that in a combined process of caffeine removal under UV irradiation and use of chitosan/TiO_2 composite membranes in phosphate-buffered medium, the photolysis mechanism is predominant, with little or no contribution from sorption, and that the TiO_2 catalyst promotes a significant reduction in the percentage of pollutant in the medium only when used dispersed and at low pH.

Keywords: photolysis; photocatalysis; caffeine; sorption

check for updates

Academic Editors: Manuel J. Chinchillas-Chinchillas, Priscy Alfredo Luque Morales and Horacio Edgardo Garrafa-Gálvez

Received: 3 June 2025
Revised: 21 July 2025
Accepted: 22 July 2025
Published: 1 August 2025

Citation: Prando, J.; Reinehr, I.L.; Visioli, L.J.; Paulino, A.T.; Enzweiler, H. Photolysis, Photocatalysis, and Sorption of Caffeine in Aqueous Media in the Presence of Chitosan Membrane and Chitosan/TiO_2 Composite Membrane. *Processes* **2025**, *13*, 2439. https://doi.org/10.3390/pr13082439

Copyright: © 2025 by the authors. Licensee MDPI, Basel, Switzerland. This article is an open access article distributed under the terms and conditions of the Creative Commons Attribution (CC BY) license (https://creativecommons.org/licenses/by/4.0/).

1. Introduction

Caffeine is found in pharmaceuticals, beverages, and foods, and is widely consumed. This organic compound is found in water bodies, resulting from wastewater, the improper disposal of medications, waste from manufacturing units, and effluents from treatment plants [1–3]. Conventional water treatment methods are not sufficient for the effective removal of caffeine, which is therefore considered an emerging pollutant that causes

concerns due to its potential risks to human health and the environment. Thus, the development of effective strategies is required for the removal of this compound from environmental sites [4–6].

Sorption and advanced oxidative processes (AOPs) have attracted attention in recent years for the removal of organic compounds from waters using UV irradiation [7,8], which is effective in the degradation of pharmaceutical products, as most such compounds are photoactive and absorb light irradiation [9]. Photolysis is one of the main AOPs that use UV light to break down large molecules into small intermediates or even achieve complete mineralization [8]. For this process to occur efficiently, the molecule must absorb a photon, and the energy of the photon must exceed the energy of the bond to be broken [10]. The presence of irradiation is crucial and strongly affects the photocatalytic degradation process [11], which is a function of the wavelength (λ) of the irradiation, the molar absorption capacity of the compounds, and the quantum yield [9]. The efficiency of the process is usually not affected by changes in temperature. Regarding light intensity, the process is significantly impacted, because the intensity of light is directly linked to the production of hydroxyl radicals (-OH), but the higher the light intensity, the less realistic the process.

Sorption techniques have a simple configuration as well as low energy and time consumption and have therefore been gaining prominence as strategies for producing effluents with low concentrations of dissolved organic compounds [6,12]. Sorption also stands out for the use of low-cost, reusable sorbents, such as chitosan and its derivatives [13]. Chitosan is the second most abundant biopolymer on Earth, behind only cellulose, and its diverse properties make it especially suitable for use in wastewater treatments [14]. The chemical structure of membranes based on this biopolymer has hydroxyl (-OH) and amino (-NH_2) functional groups that can be used as sorption sites for interaction with different pollutants in water. However, chitosan is sensitive to the pH of the solution, as are most biomaterials prepared with this biopolymer, as pH directly affects the ionization of functional groups of the chemical structure. Thus, the pH of the solution may be altered during a sorption study due to the ionization or protonation of the acidic and/or alkaline groups of the biomaterial, making the aqueous medium more acidic or alkaline in the process, which significantly interferes with the interaction between the pollutant and the sorbent material and is one of the main factors that affect the performance of a chitosan membrane [1,15,16].

Membranes synthesized with chitosan can have a three-dimensional network with high hydration capacity due to the crosslinking of the hydrophilic polymers [17]. Moreover, such membranes can have excellent sorption capacity for aqueous contaminants due to their functional groups and large available surface area [18,19]. However, one of the limitations of this type of biomaterial is the loss of mechanical strength after the swelling process [20,21]. To overcome this disadvantage, the use of crosslinking agents has been proposed as a solution to improve the permeability, chemical stability, and mechanical strength of membranes, along with increasing the sorption capacity [21–23]. Crosslinking with glutaraldehyde, in particular, improves the physical, chemical, and biological characteristics of a membrane, reducing its hydrophilicity and creating more complex structures that decrease the permeation and water absorption capacity [16,21].

AOPs have considerable potential for the removal of organic compounds from aqueous media. The theory mainly involves the formation of highly reactive, nonselective hydroxyl radicals capable of promoting the oxidation of organic matter and high reaction rates [2,24]. Heterogeneous photocatalysis stands out among the AOPs described in the literature, in which a solid semiconductor is used as the catalyst. When exposed to irradiation containing photons with energy greater than its band gap, the semiconductor absorbs the light energy, generating excited electrons (e−), which serve as oxidizing agents, and gaps (h+), which

serve as reducing agents [7]. Several factors can influence the efficiency of this process, such as the dosage of the catalyst, initial concentration of the substrate, pH of the aqueous medium, temperature of the system, power, and the wavelength of the light source [25]. The ideal pH range for many photocatalytic processes is that in which the surface charge of the photocatalyst attracts the contaminant molecules to its surface. The efficiency of the degradation process can be reduced due to the pH of the aqueous medium, the surface charge of the catalyst, and the species of the pollutant [26].

Titanium dioxide (TiO_2) is one of the most widely studied photocatalysts in AOPs. This compound is effective in the degradation of compounds such as caffeine under ultraviolet light irradiation [5,24] due to its low cost, high physical and chemical stability, hydrophilicity, and absence of toxicity [27,28]. UV irradiation causes TiO_2 to absorb photons with energy above 3.2 eV, generating highly reactive excited electrons and gaps on its surface. The photodegradation process then occurs due to the formation of free radicals and superoxides or by direct oxidation with photogenerated gaps [12,29]. The photocatalytic efficiency of TiO_2 generally depends on properties such as crystalline phase composition, particle size and morphology, surface area, and the distribution of hydroxyl groups [30]. When suspended in water, TiO_2 powder serves as a highly effective photocatalyst due to its high photonic efficiency. However, the use of free TiO_2 in photocatalysis implies additional costs for separation of the catalyst in real processes [29]. Despite the lower efficiency, the use of photocatalysts on solid supports is preferable on a large scale due to the practicality in removing pollutants and the ease of separating the catalyst from the solution at the end of the reaction. Chitosan is one of the most widely used supports [31]. Therefore, the aim of the present study was to investigate the performance of chitosan membranes and chitosan/TiO_2 composite membranes in individual and/or hybrid photolysis, photocatalysis, and sorption processes, with a focus on reaction variables, such as the pH of the aqueous medium. The main novelty of this paper is the systematic study of the contributions of different phenomena in a combined process of emerging contaminant removal by advanced oxidation using an immobilized catalyst.

2. Materials and Methods

2.1. Reagents

The reagents used in this work were analytical grade, and all aqueous solutions were prepared with distilled water. Acetic acid (CH_3COOH), monobasic sodium phosphate (NaH_2PO_4), and dibasic sodium phosphate ($Na_2HPO_4.12H_2O$) were purchased from Biotec® (Curitiba, PR, Brazil). Glutaraldehyde 50% P.A solution ($C_5H_8O_2$) was purchased from Dinâmica® (Contemporary Chemistry Ltd., Indaiatuba, SP, Brazil). Caffeine ($C_8H_{10}N_4O_2$) was purchased from Synth® (Diadema, SP, Brazil). Chitosan with a deacetylation degree of 85% and molar mass of 2.1×10^5 g mol^{-1} was purchased from Polymar® (Fortaleza, CE, Brazil). Titanium dioxide IV (TiO_2) was purchased from Neon® (Commercial Analytical Reagents LTDA, Suzano, SP, Brazil).

2.2. Synthesis of Chitosan Membranes

The membranes were prepared with chitosan (0.2 g), TiO_2 (5% in relation to the chitosan mass when the composite membranes were prepared), 0.1 mol L^{-1} acetic acid (50 mL of CH_3COOH/g of chitosan), and 1% (v/v) glutaraldehyde (6 mL of $C_5H_8O_2$/g of chitosan). The solutions were duly prepared and homogenized separately, then mixed in the appropriate proportions at room temperature under constant stirring and dispersed on silicone plates for crosslinking in an oven with forced air circulation (Fanem Orion 515) at 60 °C for 24 h. After crosslinking, the membranes were washed with distilled water to remove any impurities and then placed in the oven for another 24 h to complete crosslinking and

drying. The membranes were then stored in an environment with controlled temperature and humidity for subsequent characterization and use.

2.3. Characterization of Membranes

Fourier transform infrared (FTIR) spectra of the membranes were recorded using a Bruker Invenios-S spectrophotometer; the spectra were obtained by Attenuated Total Reflection (ATR), without using pellets, operating in the range of 400 cm^{-1} to 4000 cm^{-1}, with 32 scans per spectrum and a resolution of 4 cm^{-1}. Thermogravimetric analysis (TGA) was performed by monitoring changes in the mass of the sample during heating at a constant rate using the TGA 55 equipment (TA Instruments, Discovery series), with a heating ramp-up of 10 °C min^{-1} between 20 and 600 °C, with nitrogen flow at 60 mL min^{-1}. Differential scanning calorimetry (DSC) curves were obtained using the Netzsch DSC 200 F3 equipment in a temperature range of 0 to 600 °C, with three cycles, a heating rate of 5.0 K min^{-1}, and nitrogen flow rate of 60 mL min^{-1}. X-ray diffractograms were recorded using a Shimadzu LabX XRD-6000 diffractometer equipped with CuKα irradiation at λ 0.154 nm. The following scanning parameters were set: 2θ axis ranging from 10 to 40° and count time of 72 s for each 0.02°.

2.4. Degree of Swelling

For the determination of the degree of swelling, membrane masses of 100 mg were measured and subsequently immersed in 100 mL of aqueous medium (distilled water or buffer solutions with pH 6, 7, and 8). This system was maintained for 24 h with measurements of membrane masses in duplicate at time intervals ranging from 0 to 24 h. After each time, the membrane was removed from the aqueous medium, and excess liquid was removed, with the subsequent measurement of the mass of the swollen biomaterial on a Weblabor MG254Ai analytical scale. The degree of swelling (*DoS*) was calculated using Equation (1):

$$DoS(\%) = \left(\frac{m_t - m_d}{m_d}\right) \cdot 100 \quad (1)$$

in which m_t is the mass of the swollen membrane (g) after a given time, and m_d is the mass of the initial dry membrane (g).

2.5. Point of Zero Charge

The point of zero charge (pH_{PZC}) is the value at which the surface charge of the sorbent is considered nil [32]. To determine the pH_{PZC}, membrane masses of 0.025 g were measured and subsequently immersed in 10 mL of potassium chloride (KCl) 0.5 mol L^{-1} in glass flasks with the initial pH adjusted to 2, 4, 6, 8, 10, and 12 using sodium hydroxide (NaOH) and/or hydrochloric acid (HCl) 0.1 mol L^{-1}. The flasks were maintained at 25 °C under constant agitation using a shaker incubator (Tecnal model TE-4200) operating at 100 rpm for 24 h. The pH of the aqueous solution was then measured again—considered the final pH—using an Alfakit pH meter (model AT-355). The $pH_{initial}$ and pH_{final} were plotted on a graph, with the pH_{PZC} determined when the values on the y-axis remained constant for two or more consecutive readings [33].

2.6. Caffeine Removal Experiments

Solutions of caffeine at a concentration of 3.0 mg L^{-1} were prepared in phosphate buffer with pH values of 6, 7, and 8. A volume of 600 mL of each solution was added to a reactor containing a membrane fixed on the optical path and maintained under constant stirring at 25 °C for 15 min without the incidence of electromagnetic irradiation in order to reach the sorption–desorption equilibrium. Next, the 7 W UVC lamp (maximum emission at 254 nm) was switched, irradiating the solution with UV light for 180 min.

Aliquots of the solutions were withdrawn every 15 min and filtered in a syringe filter system with 0.22 µm pores (Syringe Filter membrane PES) prior to readings by UV-Vis spectrophotometry (BEL UV-M51 spectrophotometer) at 274 nm, within a scan of 320 to 190 nm. Under these conditions, the photolysis, photodegradation, and sorption reactions were analyzed using a membrane without a photocatalyst, a photocatalytic membrane, and a photocatalyst dispersed in the medium. The sorption of caffeine in the chitosan membrane and chitosan/TiO_2 composite membrane followed the same methodology, but without UV light irradiation. Thus, even after 15 min of sorption–desorption equilibrium, the reaction remained in the dark for 180 min. All experiments were performed in duplicate. The percentage of caffeine removal from the aqueous medium under study was calculated using Equation (2):

$$Removal\ rate(\%) = \left(1 - \frac{C_t}{C_0}\right) \cdot 100 \quad (2)$$

in which C_0 is the concentration of caffeine at time zero (soon after 15 initial minutes in the dark), and C_t is the concentration of caffeine at times greater than zero.

A summarized schematic of the processes from hydrogel synthesis to the reading of the samples is displayed in Figure 1, and each process is more detailed in Figure 2. The description of each experiment is given in Table 1.

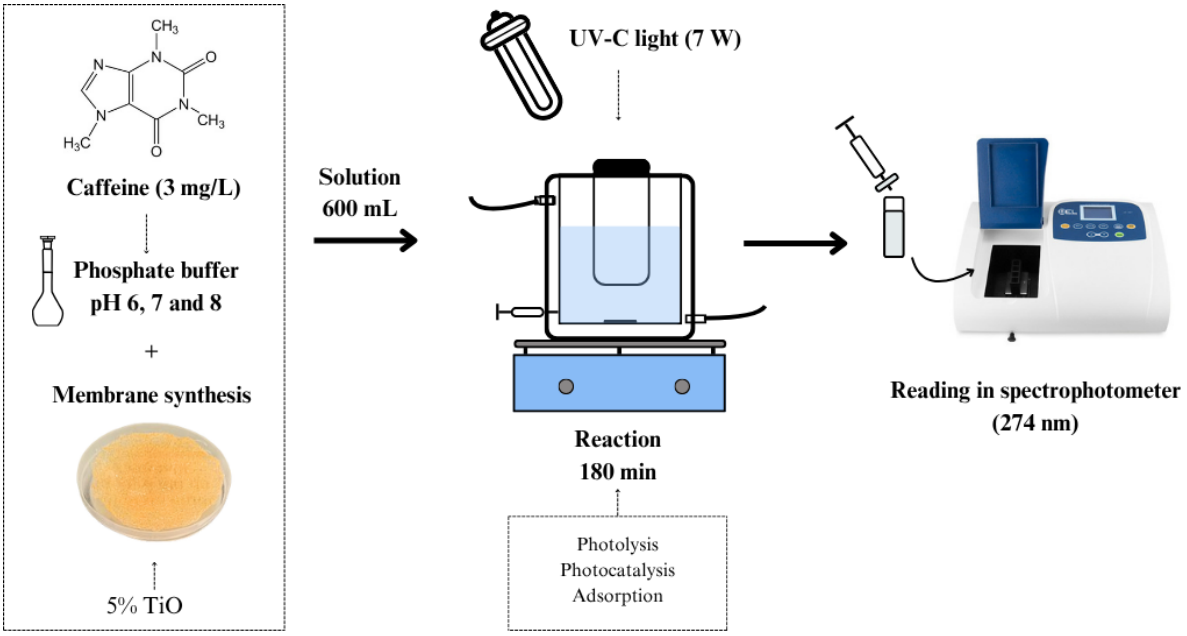


Figure 1. Illustrative schematic of caffeine removal using individual and hybrid photolysis, photocatalysis, and sorption processes.

Table 1. Description of experimental design used in the study of each of the processes of interest.

Process	Description
Photolysis	Use of irradiation source alone
Photolysis + sorption in membrane	Combined use of irradiation source and non-catalytic membrane
Sorption in membrane	Use of non-catalytic membrane in the dark
Sorption in catalytic membrane	Use of catalytic membrane in the dark
Photocatalysis with catalytic membrane	Combined use of irradiation source and catalytic membrane
Photocatalysis with dispersed catalyst	Use of catalyst dispersed in reaction medium

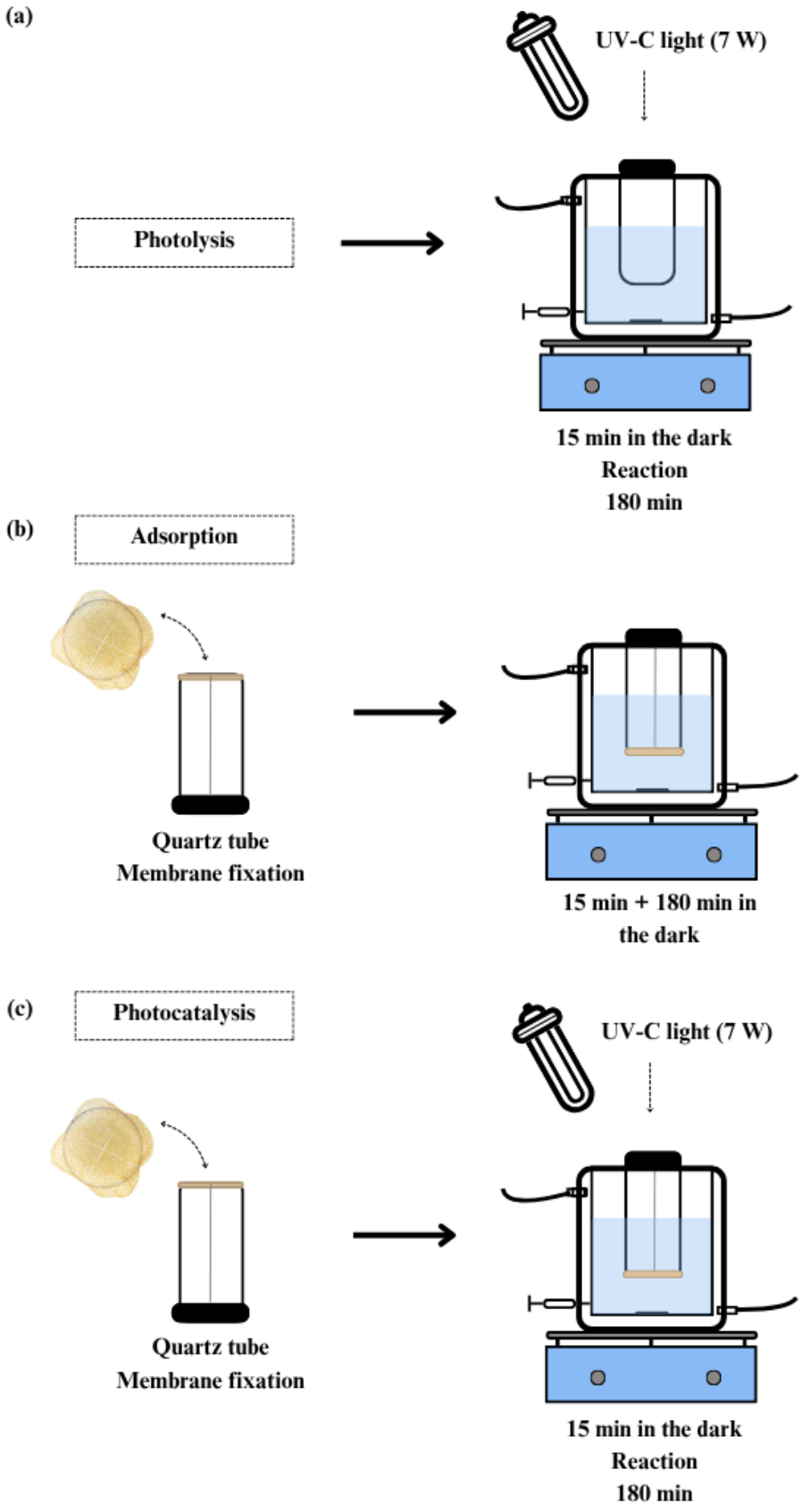


Figure 2. Illustrative schematic of caffeine removal by photolysis using UV-C light for 180 min (**a**), sorption with membrane fixed in quartz reactor with 15 min of equilibrium in the dark and 180 min of reaction in the dark (**b**), and photocatalysis with catalytic membrane fixed in quartz reactor with 15 min of equilibrium in the dark followed by 180 min of UV-C irradiation (**c**).

2.7. Reuse of the Catalytic Membrane

To evaluate the number of operational cycles supported by the chitosan/TiO_2 membrane, experiments were performed under the best photocatalysis conditions (pH 8). The analysis was conducted according to the standard procedure described above, maintaining constant reaction time, pollutant concentration, and light intensity. After completion of the photocatalysis cycle, the used membrane was carefully removed from the reactor and washed thoroughly with distilled water to eliminate residues from the reaction medium. After washing, the membrane was kept at 60 °C for 20 h in an oven to dry. The mass of the used membrane was then measured. The dried membrane was repositioned in the reactor and subjected to a new photocatalytic cycle. The washing, drying, and mass measurement procedure was repeated for three consecutive cycles, always using the same membrane. Membrane stability was monitored by the mass variation and caffeine removal efficiency throughout the reuse cycles.

2.8. Kinetics of Caffeine Removal from Aqueous Medium

The rate constant for the removal of caffeine from the aqueous medium was determined using the pseudo-zero-order kinetic model considering the batch reactor according to Equation (3):

$$C = kt + C_0 \quad (3)$$

in which C is the concentration of caffeine, k is the pseudo-zero order rate constant, t is the reaction time, and C_0 is the concentration of the pollutant at the beginning of the reaction.

2.9. Statistical Analysis

The experimental values are expressed as mean ± standard deviation of duplicate experiments. The data were analyzed using ANOVA, followed by Tukey's test to determine multiple differences among groups using Excel. The minimal significant difference (MSD) was calculated using Equation (4):

$$MSD = q\sqrt{\frac{QMR}{2}} \quad (4)$$

in which QMR is the residual standard deviation, and q is the tabulated value of Tukey's test with 95% confidence.

QMR was calculated using Equation (5):

$$QMR = \frac{SQ_{res}}{GL_{res}} \quad (5)$$

in which SQ_{res} is the sum of square of the residuals that measures the variation within groups, and GL_{res} regards the degrees of freedom associated with the residuals.

3. Results and Discussion

3.1. Characterization of Chitosan Membranes

3.1.1. FTIR Spectra

Figure 3 displays FTIR spectra for chitosan membrane, chitosan/TiO_2 composite membrane before caffeine removal process, and chitosan/TiO_2 composite membrane after caffeine removal tests at pH 6, 7, and 8.

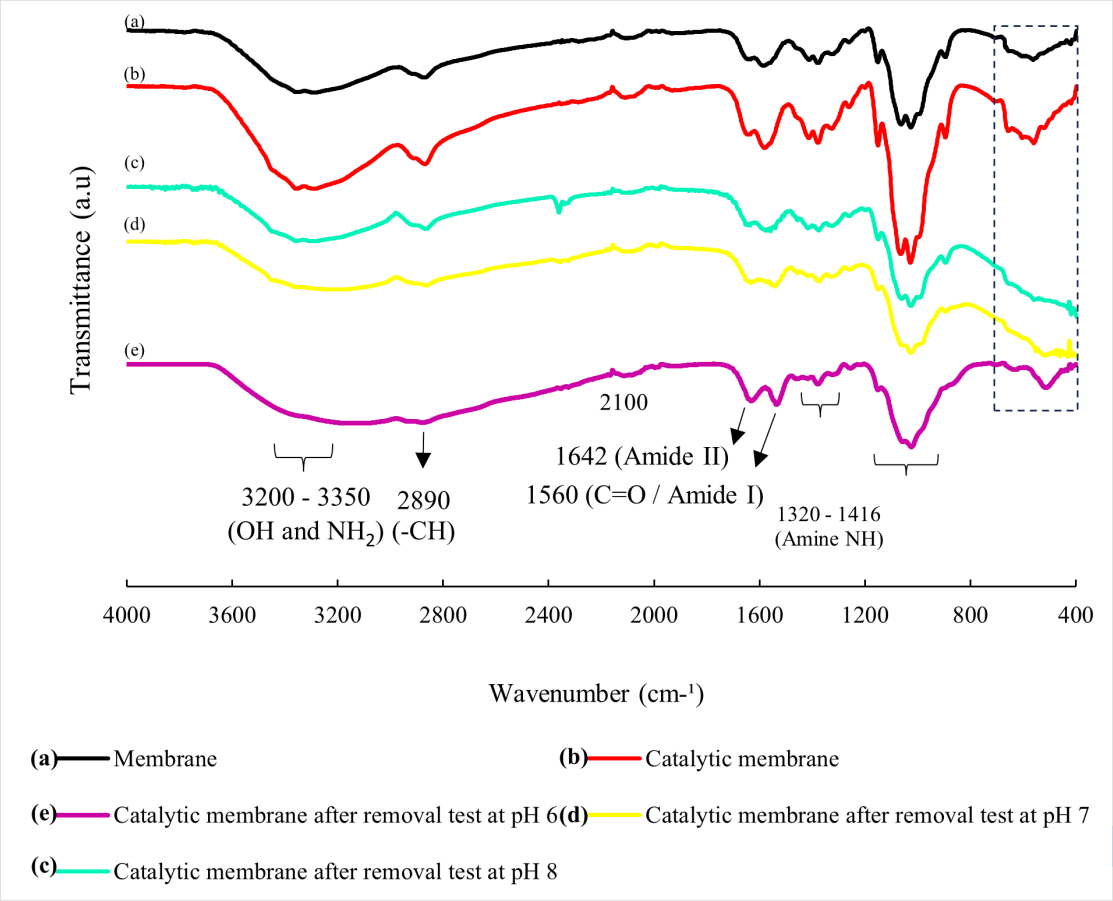


Figure 3. FTIR spectra for chitosan membrane, chitosan/TiO_2 composite membrane before caffeine removal process, and chitosan/TiO_2 composite membrane after caffeine removal tests at pH 6, 7, and 8.

The absorption bands between 3350 and 3200 cm^{-1} are attributed to the elongation and/or stretching of chemical bonds involving hydroxyl groups (OH) and amino groups (NH_2) in the chitosan macromolecule. These groups are affected when water is adsorbed to the structure of the polymeric biomaterial [19,27,34]. The absorption bands at 2890 cm^{-1} correspond to the elongation of aliphatic groups [32], whereas those found between 1600 and 800 are related to the chemical composition of chitosan [35]. The bands between 1642 and 1560 cm^{-1} and those between 1416 and 1320 cm^{-1} indicate the presence of primary and secondary amide groups that appear due to the crosslinking of chitosan with a high degree of deacetylation [36–38]. The covalent bond between amine groups of chitosan and aldehydes from the crosslinking agent (C=N) can be observed in the band at 1642 cm^{-1}. The formation of amine groups, through Schiff base reactions, indicates a successful crosslinking between chitosan and glutaraldehyde [39,40]. Signs of vibrations of hydroxyl groups derived from water molecules absorbed in the structures of the membranes were also seen between 1660 and 1550 cm^{-1} [37]. The bands in the region between 1113 and 896 cm^{-1} were attributed to the saccharide structure of the chitosan macromolecule [36]. Lastly, the absorption band at 1073 cm^{-1} was attributed to the stretching of C–O–C bonds. Changes in the intensities of the absorption bands were found after the incorporation of TiO_2 into the structure of the chitosan membrane during the synthesis of the composite membrane, indicating the interaction between OH groups and TiO_2 in the biopolymer network [41,42]. The absorption bands that appear below 1000 cm^{-1} (region highlighted by dashed rectangle) in the chitosan/TiO_2 composite membranes were attributed to charac-

teristic signals of Ti–O bonds [27]. The increase in intensity at 570 and 560 cm^{-1} suggests interactions between Ti-O-Ti and chitosan functional groups [12,27]. As TiO_2 tends to enter mainly the amorphous region of chitosan during the synthesis of the composite membrane, the formation of strong hydrogen bonds is indicated at 3300 cm^{-1} [43]. In this case, numerous variations in absorption band intensities between the chitosan membrane and chitosan/TiO_2 composite membrane may be associated with the occupation of active sites in biopolymer networks [44]. In such cases, the photocatalyst remains incorporated in the membrane without affecting the chemical structure of chitosan due to the occurrence of physical deposition in the pores of the biomaterial [45]. Comparing the FTIR spectra of the catalytic membrane after the removal tests at pH 6, 7, and 8, shifts and changes in some bands are identified, resulting from the interaction of caffeine and species of the buffer with the membrane. This is evident in the bands between 3350 and 3200 cm^{-1} as well as the band at 2890 cm^{-1}, where interactions occur between OH, NH_2, and CH available in chitosan and phosphate ions and sodium ions from the buffer solution [46,47]. The band shift at 890 cm^{-1} and the band shift at 1018 cm^{-1}, corresponding to the P-O bond, indicate that the hydroxyl groups were replaced by surface-adsorbed phosphate [48–50]. The signals at 1024 and 507 cm^{-1} are additional evidence of the presence of phosphate sorbed in the membrane structure [51]. Moreover, the TiO_2 absorption bands at pH 6, 7, and 8 are overlapped by other bands that appear in the spectra. Interaction of phosphate with these groups, mainly with the shift of the band present between 570 and 560 cm^{-1} to a more explicit vibrational mode close to 507 cm^{-1} was found after the caffeine removal study at pH 6, indicating the presence of the O-P-O group [52]. Comparing the spectra after the caffeine removal tests, the shifts and changes in the absorption bands become more evident as the pH becomes more acidic, indicating greater interaction between caffeine and the buffer ions in the membrane structure. Thus, pH is important to the occurrence of intermolecular and intramolecular interactions between chemical species in the solution and the solid molecular structure of the biopolymeric membrane.

3.1.2. TGA and DSC

The first evidence of thermal degradation for the chitosan membrane and chitosan/TiO_2 membrane can be seen in Figure 4.

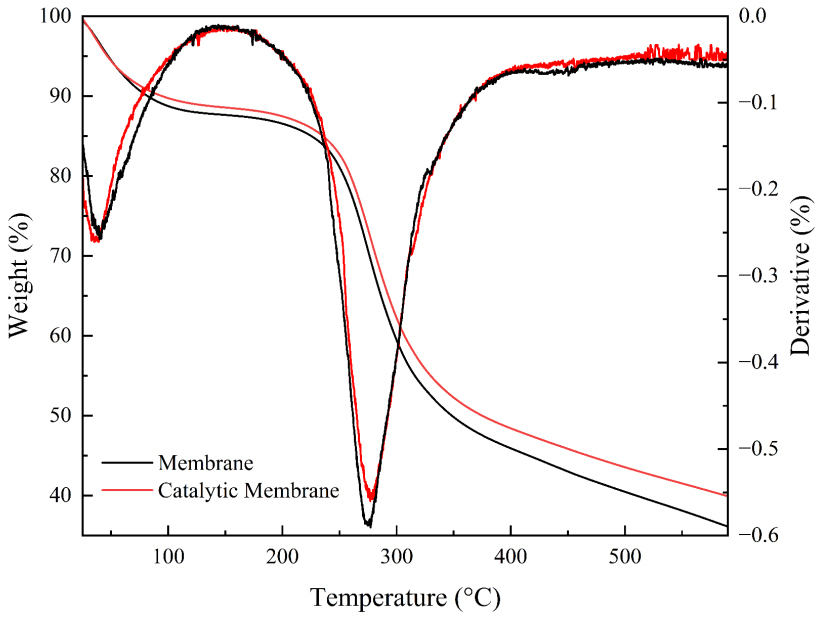


Figure 4. Results of thermogravimetric analysis (TGA) and differential thermogravimetric analysis (DTG) for chitosan membrane and chitosan/TiO_2 composite membrane.

The TGA curves show the loss of mass as a function of temperature and the DTG curves show the peaks that indicate the maximum degradation temperature for each sample. Approximately 10% loss of mass occurred between 80 and 150 °C due to the evaporation of water can be present even after the drying process. At these temperatures, mass loss may also occur due to the acetic acid residue used for the solubilization of chitosan [32,34,53]. The second phase of degradation occurred between 230 and 400 °C, which is related to the decomposition of polymeric monomers and the break of glycosidic bonds. A clear peak was observed around 270 °C, as indicated by the DTG curves [19,34,37]. The greater loss of mass after 450 °C occurs due to the efficiency of the thermal decomposition of most polymeric biomaterials at high temperatures [37]. A slightly greater loss of mass of the chitosan membrane was found compared to the composite membrane after increasing the temperature. The reduction in the mass of the chitosan membrane and composite membrane was 64% and 60% at 600 °C. This occurs because more pores with empty volumes are found in the biopolymer network of the membrane without the presence of compounds such as TiO_2, facilitating the diffusion of solutes and minimizing intermolecular interactions, which diminishes thermal stability. When compounds are incorporated into the biopolymer network during the formation of composite materials, an increase can occur in the degree of crosslinking, and there may be a smaller number of pores, thus increasing the rigidity of the final material [35,41,54]. The DSC results for the chitosan membrane and chitosan/TiO_2 composite membrane are shown in Figure 5.

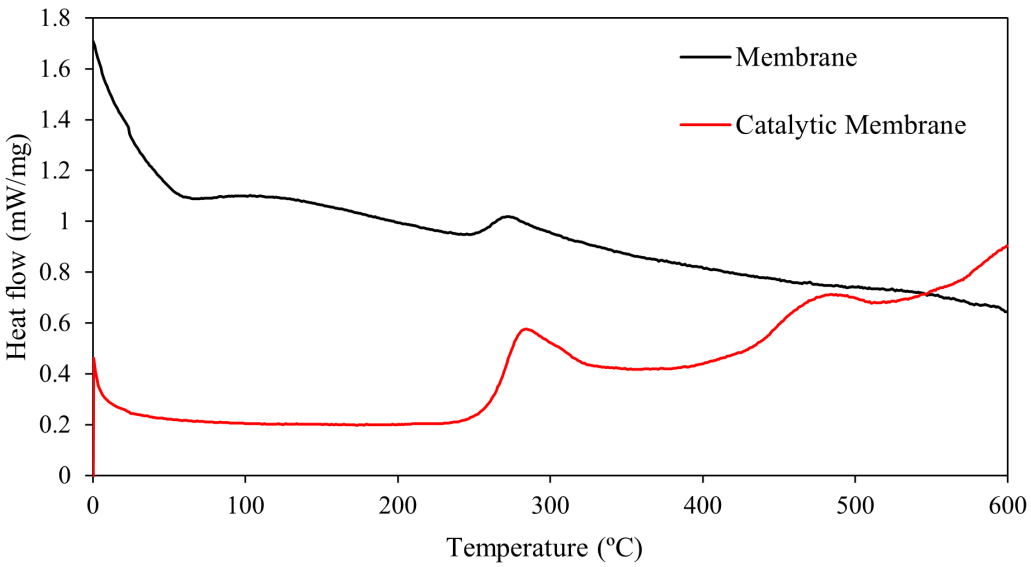
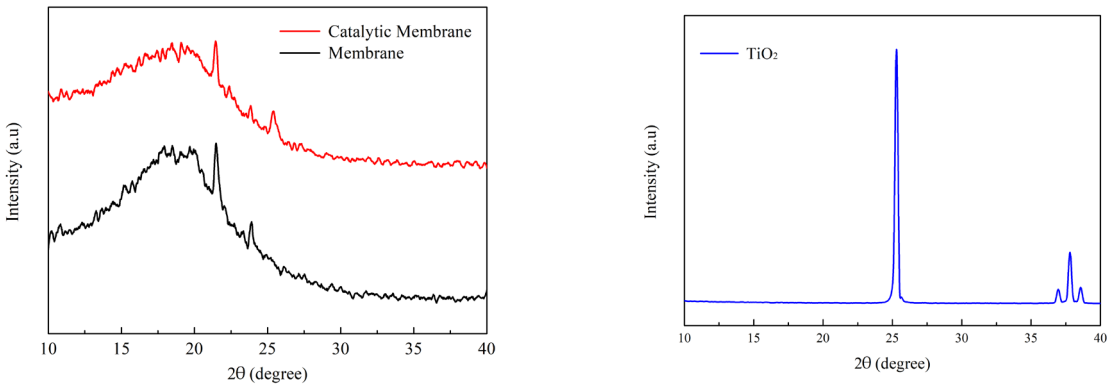


Figure 5. Results of differential scanning calorimetry for chitosan membrane and chitosan/TiO_2 composite membrane.

An endothermic peak was found in the first phase of thermal degradation close to 60 °C due to the loss of water [54], which is in agreement with the TGA and DTG results. Exothermic peaks for the chitosan membrane and chitosan/TiO_2 composite membrane were found at 275 and 288 °C, respectively, due to the thermal decomposition of the biopolymer. In this case, dehydration of saccharide rings occurs, followed by the decomposition of the main structure of chitosan [54–56]. Exothermic peaks were also found at ~460 °C due to the decomposition of units of acetyl groups [38]. These results are also in agreement with those found in the TGA and DTG curves, indicating that the presence of TiO_2 in the membrane network, even in small concentrations, contributes to improving the thermal stability of the final material.

3.1.3. X-Ray Diffractograms

The X-ray diffractograms for the chitosan membrane and chitosan/TiO_2 composite membrane are displayed in Figure 6.



(**a**) (**b**)

Figure 6. (**a**) X-ray diffractograms for chitosan membrane and chitosan/TiO_2 composite membrane and for (**b**) TiO_2 powder.

Peaks of the same intensity were recorded at 2θ ~18° (110) and 21.4° (111), indicating that the characteristic amorphous structure of chitosan did not undergo changes with the addition of the photocatalyst in the final biopolymer network [57]. The peak at 25.3° (101) in the composite membrane regards the presence of TiO_2, mainly in the anatase phase [58]. Peaks in these regions suggest the presence of a biocomposite structure with certain crystallinity compared to the conventional membrane and are characteristics of chitosan molecules that aligned due to intermolecular interactions during the formation of the biomaterial [32,35,59,60]. The wider bands between 19.0 and 25.0° confirm the presence of amorphous structures during the crosslinking reactions [61].

3.1.4. Degree of Swelling

The degrees of swelling of the chitosan membrane and chitosan/TiO_2 composite membrane are displayed in Table 2.

Table 2. Degree of swelling of chitosan membrane and chitosan/TiO_2 composite membrane in water and different aqueous buffer solutions at pH 6, 7, and 8.

Sample	Degree of Swelling (%)			
	H_2O	pH 6	pH 7	pH 8
Chitosan	481.59 ± 74.26 ^{a}	138.20 ± 6.51 ^{b}	171.17 ± 40.92 ^{b}	180.50 ± 38.53 ^{b}
Composite	376.25 ± 8.31 ^{a}	115.42 ± 10.11 ^{c}	158.81 ± 7.77 ^{b}	131.20 ± 5.95 ^{b}

Same letters denote statistical similarity of samples with variation of the solution. Data expressed as mean and standard deviation, with 95% confidence according to Tukey's test.

The degrees of swelling of the membranes immersed in distilled water were between 30 and 40% higher than those determined in buffer solutions at pH 6, 7, and 8. This may be attributed to the greater availability of free water molecules in the absence of a buffered solution, which facilitates the diffusion and expansion of the polymer matrix [19,62]. Cations and anions from buffer solutions can occupy active interaction sites in the membrane structure, hindering hydration. The degree of swelling was lower at pH 6 compared to pH 7 and 8 due to the variation in the ionic structure of the biomaterial and the higher concentration of ions in the solutions. The addition of a photocatalyst to the membrane influenced the

swelling properties of the material, as TiO_2 has the ability to form hydrogen bonds with chitosan, thus limiting the interaction with water molecules [41–43]. The reduction in the degree of swelling of the composite membrane compared to the membrane without the catalyst was 22, 17, 7, and 28% in water and buffer solutions at pH 6, 7, and 8, respectively. A lower degree of swelling can limit the material with regard to the absorption of fluids [63]. This behavior may be related to the stabilization of intermolecular interactions in the presence of buffer ions. The swelling mechanism of a biomaterial in aqueous medium is dependent on water diffusion and the stability of the polymer structure. The migration of water weakens the hydrogen bonds between the chemical groups of the polymer network with an increase in the expansion and size of the final material [38]. Lastly, the degree of swelling is affected by the hydrophilicity, rigidity, and porous structure of the biomaterial. Samples with a higher degree of swelling generally have a larger surface area and volume and may have less mechanical strength [64].

3.1.5. Point of Zero Charge (pH_{PZC})

The pH_{PZC} on the surface of the chitosan membrane was 7.1. After the caffeine sorption studies, the pH_{PZC} of the same membrane was 6.4, 6.9, and 7.8 at pH 6, 7, and 8, respectively (Figure 7).

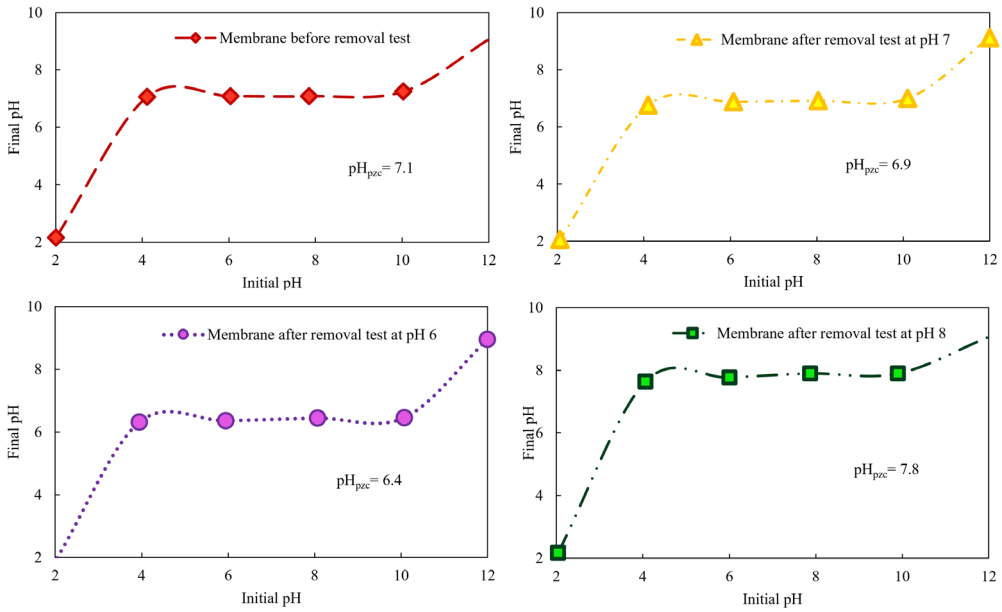


Figure 7. Point of zero charge (pH_{PZC}) for chitosan membrane before and after caffeine sorption studies at different pH values.

These results indicate that the degree of ionization and the charge of the surface of chitosan depend on the pH of the medium [65,66] and are significantly affected by the ions of the buffer solution. The surface of the membrane is negatively charged when immersed in solutions with pH above the pH_{PZC}. In this case, the excess of anionic groups facilitates the sorption of cations. In contrast, the biomaterial is positively charged when immersed in solutions with pH values below the pH_{PZC}, protonating groups such as amine [32,67]. It is possible to infer that the membrane surface is predominantly charged with positive groups after the sorption tests at pH 6 and 7, which is useful for the sorption of anions, whereas the membrane is predominantly charged with negative groups at pH 8, which is useful for the sorption of cations. Thus, one may study the selective sorption of cations and anions in aqueous media depending on the pH. The excess of chemical groups with the same charges in the reaction media generates electrostatic repulsion forces between sorbates and sorbents, whereas chemical groups with different charges generate electrostatic attraction forces [37].

As the caffeine molecule tends to be negatively charged at high pH values and positively charged at low pH values [68], it is possible to optimize the sorption of this compound to obtain better removal capacities by varying the pH.

3.2. Caffeine Removal from Water

The removal of caffeine from water was performed in individual and hybrid processes involving photolysis, sorption, and photodegradation. All these tests were performed in duplicate and at three pH values (6, 7, and 8). The results indicated a linear relationship between concentration and time, suggesting pseudo-zero-order kinetics. The removal rate constants for photolysis, sorption, photocatalysis, and hybrid processes with varying pH are displayed in Table 3.

Table 3. Rate constant (k) and respective standard errors for individual and hybrid photolysis, sorption, and photocatalysis processes using chitosan membrane and chitosan/TiO_2 composite membrane with different pH values.

Process	k Values (mg $L^{-1}h^{-1}$)		
	pH = 6	pH = 7	pH = 8
Photolysis	0.063 ± 0.004^{Ba}	0.093 ± 0.013^{Aa}	0.111 ± 0.030^{Aa}
Photolysis + sorption	0.081 ± 0.004^{Ba}	0.084 ± 0.017^{Aa}	0.114 ± 0.008^{Aa}
Sorption in chitosan membrane	0.008 ± 0.005^{Ca}	0.015 ± 0.004^{Ba}	0.010 ± 0.011^{Ba}
Sorption in composite membrane	0.014 ± 0.014^{Ca}	0.027 ± 0.013^{Ba}	0.001 ± 0.000^{Ba}
Photocatalysis with composite membrane	0.060 ± 0.008^{Bb}	0.075 ± 0.004^{Aa}	0.108 ± 0.017^{Aa}
Photocatalysis with dispersed catalyst	0.366 ± 0.034^{Aa}	0.111 ± 0.004^{Ab}	0.105 ± 0.004^{Ab}

Same uppercase letters [A, B, C] denote statistical similarity for processes with constant pH. Same lowercase letters [a, b] denote statistical similarity for processes with variation in pH. Data expressed as means with 95% confidence according to Tukey's test.

The caffeine removal rate from water via photolysis was 85% higher than that determined for membrane sorption. The means of caffeine removal percentage after 180 min of treatment with respective standard deviations and statistical similarity, according to Tukey's test with 95% confidence, are shown in Figure 8.

The presence of a photocatalyst in the chitosan membrane structure did not significantly increase the caffeine removal percentage. However, a slightly lower removal was found at pH 7. When the catalyst was used dispersed in the aqueous medium, a higher caffeine removal was found at pH 6 compared to the other pH values.

The removal during the photolysis reactions were 19.50 ± 1.14, 28.61 ± 0.05, and 30.64 ± 6.32% at pH 6, 7, and 8, respectively. The nonsignificant difference between pH 7 and 8 suggests that irradiation alone could lead to high-level oxidation of the compound of interest [69]. However, it is often still insufficient for real applications. Therefore, it is important to investigate hybrid processes, such as those proposed in this study.

In photolysis, the most commonly used irradiation has a wavelength in the range of 200 to 400 nm (UV spectrum region), and the degradation of the molecule depends on the absorption capacity of this incident irradiation to reach an excited state and promote the breaking of bonds. However, the likelihood that the excited state results in photolysis is governed by the quantum yield [70]. The high removal rates in the photolytic reactions is explained by the use of a UVC lamp with a low wavelength (peak at 254 nm), in which photon emission occurs with high energy [71,72]. If the molecule is not degraded directly by photolysis, indirect degradation may occur due to the formation of hydroxyl radicals from the water [9].

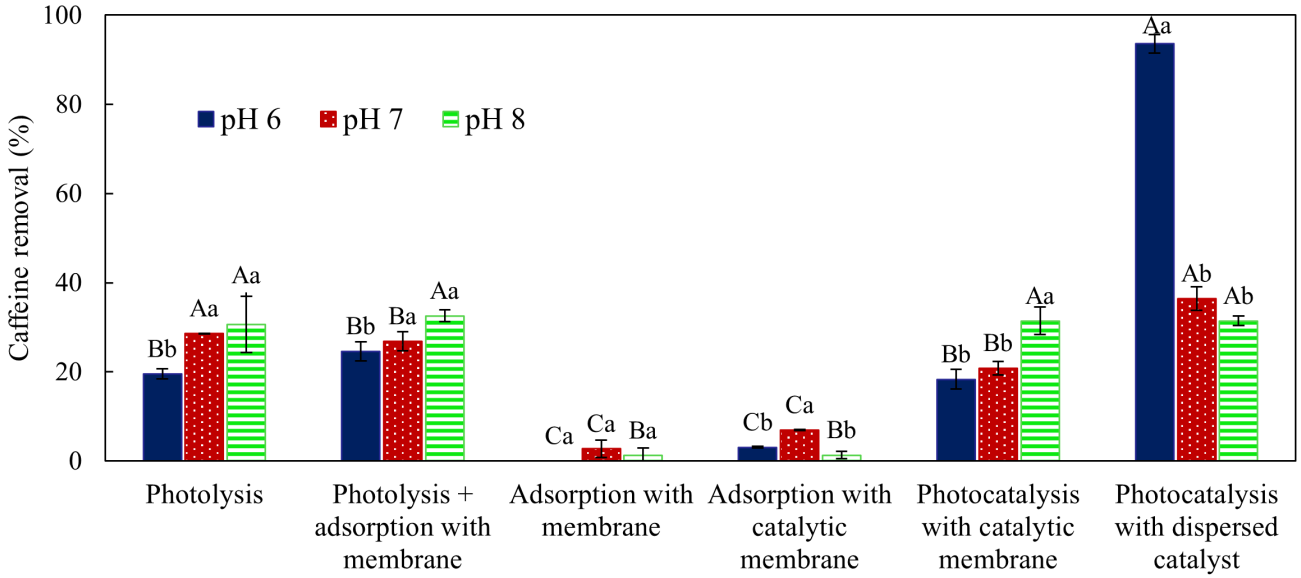


Figure 8. Caffeine removal percentages from water in different processes and pH values. Same uppercase letters [A, B, C] denote statistical similarity for processes with constant pH. Same lowercase letters [a, b] denote statistical similarity for processes with variation in pH. Data expressed as means with 95% confidence according to Tukey's test. So, capital letters compare different processes at fixed pH, and lowercase letters compare pH variation for a given process.

For caffeine sorption in the chitosan membrane, removal percentages were 2.73 ± 1.96 and 1.21 ± 1.71% at pH 7 and 8, respectively, whereas no removal occurred at pH 6, indicating that the membrane practically did not adsorb caffeine. The removal profile remained constant throughout the 3 h test, with small increases at some points and greater stabilization after 60 min, indicating sorption equilibrium. This is in agreement with some results previously reported for other types of biomaterials studied for caffeine sorption in aqueous media [73]. As chitosan has hydroxyl and amino groups in its chemical structure, which serve as efficient active sites for sorption [74], the poor performance may be attributed to the surface properties of the sorbent and sorbate. The difficulty in the removal of caffeine from aqueous media using chitosan biomaterials may also be associated with the alkaline nature of this compound, which has greater ionization difficulty at milder pH values [75]. Another factor that may interfere with caffeine sorption is the hydrophilic nature of the chitosan membrane and the hydrophobic nature of caffeine, as both tend to disfavor intermolecular and intramolecular interactions between two species [76].

When considering sorption, it is also necessary to infer that changes in the pH of the solution interfere with the surface charge of the sorbent, along with the presence of species other than that of interest in the study medium [77,78]. The variation in pH and presence of chemical species in the solution during a sorption process can be interpreted by analyzing the pKa and pH_{PZC}. For instance, the pKa of the caffeine molecule is 10.4, which means that the molecule is fully protonated at a pH lower than this value and deprotonated at a higher pH [79]. Thus, the structure of the chitosan membrane and the protonated caffeine at the pH values studied impede electrostatic attraction, which affects the removal capacity [73]. In the pH range studied, the main species in the buffer are monovalent $H_2PO_4^-$ (pH between 3.0 and 7.20) and HPO_4^{2-} (pH between 7.20 and 10.0) [67]. At neutral pH, OH is the main reactant [80]. As the pH increases, the amount of OH ions increases, thus diminishing the likelihood of phosphate ion sorption [77,81]. At pH below 6.3 (pKa of the chitosan membrane) [32,37,78], glucosamine (NH_2) units are converted, forming -NH^{3+} ions. This increases the electrostatic repulsion forces in the presence of the caffeine buffer solution, diminishing the sorption capacity, as observed experimentally [44].

The sorption percentages in the chitosan/TiO_2 composite membrane were 6.93 ± 0.16, 3.06 ± 0.21, and 1.31 ± 0.82% at pH 6, 7, and 8, respectively. The sorption percentage and profile were similar to those found using the chitosan membrane, as TiO_2 achieves relatively low sorption for most pollutants [82]. Irrespective of the concentration of the photocatalyst, mass transfer limitations to the photocatalyst surface occur in sorption experiments [7,28] due to the protonation or deprotonation capacity with the variation in pH [35,83]. The combined effects of photolysis and sorption with the non-catalytic membrane reinforce the impact of UV irradiation on caffeine removal. The main advantages of photolysis over non-photochemical degradation include the non-use of chemical reagents, the reduction in oxidants, and the lower impact on variations in pH [9]. Analyzing the caffeine removal percentages of 24.62 ± 2.14, 26.85 ± 2.12, and 32.56 ± 1.34% after 180 min at pH ranging from 6 to 8, it can be inferred that the membrane interfered in photolysis when pH = 7 was used, as there was a decrease in caffeine removal when compared to the reaction with UV irradiation alone (photolysis). This occurs because pH effects tend to be more significant when greater than 6.5 (pKa of amine groups in chitosan molecules) [32], promoting the formation of hydroxyl radicals and affecting the sorption and degradation process [83,84].

The caffeine removal percentages from the aqueous media were 93.56 ± 2.12, 36.42 ± 2.59, and 31.41 ± 1.07% at pH 6, 7, and 8, respectively, using the dispersed catalyst in the presence of UV irradiation. A growing linear profile was found throughout the photocatalytic removal process as the pH decreased. These results are in agreement with previous findings described in the literature for the photocatalysis of caffeine using a 16 W low-pressure Hg-UV lamp at different pH values. This is an indication that the degradation was better in acidic conditions due to the surface charges [75]. In photocatalytic activity processes using a free catalyst, it is common for a decrease in the removal percentages to occur at high pH values due to the precipitation of metal hydroxides, which diminishes the concentration of hydroxyl radicals formed [32]. The pH of the medium also affects the surface charge of the photocatalyst and the ionization of caffeine molecules in the solution [79]. Another important factor that affects the process is that the dominant species in the phosphate buffer changes to HPO_4^{2-} at pH above 7.2. Phosphate ions have strong interactions with H_2O through hydrogen bonds and acid-based reactions, considerably accelerating the oxidation pathway by hydroxyl radicals. However, this hinders the interaction between the pollutant and TiO_2, suppressing the direct electron transfer pathway [85]. The stability and solubility of the photocatalyst, which in turn impact the duration and effectiveness of caffeine removal, can also be influenced by pH [26]. Although the dispersed catalyst has high activity at pH 6 due to the larger surface area, it is not easily separated from the treated solution [85]. Thus, when viable, the use of an immobilized catalyst is preferable.

The caffeine removal percentages using the photocatalytic membrane in the presence of UV irradiation were 18.33 ± 2.20, 20.83 ± 1.49, and 31.41 ± 3.08% at pH 6, 7, and 8, respectively, after 180 min of reaction. Compared to the previous results, one can infer that the catalyst is not on the surface of the membrane for photocatalytic oxidation to occur in a facilitated manner and that removal only occurs through the action of the UV light (photolysis). Thus, organic contaminants in the water are first sorbed on the surface of the immobilized TiO_2 and then oxidized by the electron gap (h+) and/or •OH in the photocatalytic oxidation reaction [29,42]. Degradation tests of compounds using TiO_2 in the form of anatase and a zeolite/TiO_2/H-beta composite catalyst generated better results. In this case, TiO_2 was better distributed on the surface of the composite, resulting in more active sites for contact with caffeine [75]. Thus, it can be said that the hydrogel catalytic membrane in the present study was influenced by the buffer solution, in addition to not having an affinity for caffeine.

Caffeine removal tests were performed using the TiO_2 catalytic membrane in a medium containing only deionized water, with a degradation percentage activated of 53.04 ± 0.89%, confirming the effect of buffer solution. Although it is important to highlight that the test in pure water had a significant change in pH over time (from 6.2 to 4.9), a factor that, as mentioned previously, can change the surface charges and affect the degree of ionization. Zhao suggests that modifying the TiO_2 surface with phosphate ions can favor the oxidative route via hydroxyl radicals (•OH); however, this modification tends to hinder direct oxidation by holes (h^+) and the interaction of the catalyst with the pollutant, altering the overall mechanism of the photocatalytic process and, in this case, having a negative effect on removal [84].

The tests performed to evaluate the resistance of the catalytic membrane during reuse showed removals of 32.96, 23.82, and 22.32% for the first, second, and third treatment cycles, respectively. The reuse efficiency was 86.80 and 86.67% for the second and third cycles, when compared to the pollutant removal in the first cycle. The reason for the reduction in photoactivity may be related to the decreased availability of active sites for sorption and photocatalytic reaction [86]. Regarding physical stability, a mass loss of 27.73% was recorded between the first and second cycles and 4.55% between the second and third cycles, suggesting good reuse potential of the catalytic membrane in the reaction medium studied.

Positive and negative groups on the surfaces of solid supports prepared with biopolymers, such as chitosan, can alter the interaction between light and immobilized catalysts, affecting the efficiency of photodegradation [11,32]. When the pH of the solution increases, the degree of ionization of chitosan decreases, and less diffusion of the buffer within the biopolymer occurs [65]. Moreover, the occupation of the surface by phosphate anions can be competitive with the sorption of organic molecules and the formation of hydroxyl radicals, affecting the photocatalytic degradation of the pollutant [85]. Some studies have also reported that the point of zero charge of TiO_2 particles is significantly shifted to a lower pH value in the presence of the phosphate anion [79]. This indicates an accumulation of negative charges on the surface of the photocatalyst, which can form a negative electrostatic field in the surface layer and promote the separation of electrons and gaps.

The presence of natural organic materials and other real residual contaminants can impact the efficiency and selectivity of membranes, as it can act through one of three main mechanisms: (i) competition for active sites and light attenuation [87], (ii) compromising of the reaction mechanisms [88], or (iii) change in selectivity [89]. Nevertheless, all these interferences are mitigated through conventional treatments, such as coagulation and filtration, which ultimately remove most of the compounds that could compromise process efficiency, which would be classified as tertiary effluent treatment.

Through absortion scanning during the reactions and parallel studies, it was possible to observe the presence of some caffeine processing intermediates in a very low concentration. These intermediates are formed possibly by N-demethylation and hydroxylation reactions, generally mediated by hydroxyl radicals (•OH). The most probably intermediates are theobromine (3,7-dimethylxanthine) and paraxanthine (1,7-dimethylxanthine) [90]. Depending on their occurrence, and particularly when using the membrane, the presumable formation of uric acid and carboxylic acid could be observed. All these compounds are less toxic than caffeine and are less persistent in the environment [91].

Analyzing all the processes individually (photolysis, photocatalysis, and sorption) and the hybrids studied, one can infer that UV irradiation alone may be sufficient to reduce the concentration of the pollutant in the environment, as the UVC lamp emits a large quantity of high-energy photons. However, caffeine has little affinity for the chitosan membrane due to its different physicochemical properties. One must bear in mind that caffeine is hydrophobic and its chemical groups have high pKa values, whereas the chitosan

membrane is hydrophilic and has a pKa of around 6.5. Differences in pKa can generate electrostatic repulsion forces between caffeine and the membrane, impeding sufficient approximation of both for removal.

4. Conclusions

The physicochemical properties of the chitosan membrane are positively influenced by the addition of the catalyst in the formation of the composite biomaterial, as demonstrated by FTIR, TGA, DSC, XRD, and the degree of swelling. The change in the pH of the solution affects the membrane surface and influences the degree of swelling, pH_{PZC}, and caffeine removal percentage. The use of buffer contributed to a lower degree of swelling and change in the pH_{PZC}. In the hybrid process, photolysis was the process with the greatest contribution to caffeine removal, as the sorption of the compound indicated lower removal rates, irrespective of whether the membrane was catalytic or not. These results indicate that buffer ions can exert an influence on the surface charge of the membrane and the occupation of active sites during the removal tests, interfering with the breakdown of the caffeine molecule in hybrid processes. It is also clear that, despite the advantages arising from the use of immobilized TiO_2, the pH conditions of the reaction medium must be assessed carefully when the chitosan membrane is used.

Author Contributions: Formal analysis, data curation, J.P.; formal analysis, data curation, I.L.R.; resources, supervision, funding acquisition, L.J.V.; resources, funding acquisition, visualization, writing—review and editing, A.T.P.; conceptualization, project administration, funding acquisition, writing—original draft preparation, H.E. All authors have read and agreed to the published version of the manuscript.

Funding: This research was funded by Fundação de Amparo à Pesquisa e Inovação do Estado de Santa Catarina, FAPESC—Brazil, grant numbers 2021/TR001810, 2023/TR331, and 2024TR002572; Conselho Nacional de Desenvolvimento Científico e Tecnológico, CNPq, Brazil, grant number 313064/2022-9; and Coordenação de Aperfeiçoamento de Pessoal de Nível Superior, CAPES, Brazil—Finance Code 001.

Data Availability Statement: The original contributions presented in this study are included in the article. Further inquiries can be directed to the corresponding author.

Acknowledgments: H.E. thanks Fundação de Amparo à Pesquisa e Inovação do Estado de Santa Catarina (FAPESC, Brazil) for the financial support (Grant number: 2021/TR001810). A.T.P., H.E., and L.J.V. thank FAPESC, Brazil for the financial support (Grant numbers: 2021/TR791, 2023/TR331, and 2024TR002572). A.T.P. thanks Conselho Nacional de Desenvolvimento Científico e Tecnológico (CNPq, Brazil) for the research productivity fellowship (Grant number: 313064/2022-9). This study was also funded in part by Coordenação de Aperfeiçoamento de Pessoal de Nível Superior (CAPES, Brazil—Finance Code 001).

Conflicts of Interest: The authors declare no conflicts of interest.

References

1. Gonçalves, J.O.; Strieder, M.M.; Silva, L.F.O.; dos Reis, G.S.; Dotto, G.L. Advanced Technologies in Water Treatment: Chitosan and Its Modifications as Effective Agents in the Adsorption of Contaminants. *Int. J. Biol. Macromol.* **2024**, *270*, 132307. [CrossRef] [PubMed]
2. Arfanis, M.K.; Adamou, P.; Moustakas, N.G.; Triantis, T.M.; Kontos, A.G.; Falaras, P. Photocatalytic Degradation of Salicylic Acid and Caffeine Emerging Contaminants Using Titania Nanotubes. *Chem. Eng. J.* **2017**, *310*, 525–536. [CrossRef]
3. de Oliveira, C.P.M.; Sperle, P.; Arcanjo, G.S.; Koch, K.; Viana, M.M.; Drewes, J.E.; Amaral, M.C.S. Successful Application of Photocatalytic Recycled TiO_2-GO Membranes for the Removal of Trace Organic Compounds from Tertiary Effluent. *Chemosphere* **2024**, *362*, 142730. [CrossRef]

4. da Silva Vasconcelos de Almeida, A.; Vieira, W.T.; Bispo, M.D.; de Melo, S.F.; da Silva, T.L.; Balliano, T.L.; Vieira, M.G.A.; Soletti, J.I. Caffeine Removal Using Activated Biochar from Açaí Seed (*Euterpe oleracea* Mart): Experimental Study and Description of Adsorbate Properties Using Density Functional Theory (DFT). *J. Environ. Chem. Eng.* **2021**, *9*, 104891. [CrossRef]
5. Mergenbayeva, S.; Zakharova, A.; Tynysbek, A.; Koole, L.H.; Atabaev, T.S.; Poulopoulos, S.G. Polymer Immobilized TiO_2 Microparticles for Photocatalytic Degradation of Caffeine. *Mater. Today Proc.* **2022**, *71*, 119–123. [CrossRef]
6. Zanella, H.G.; Spessato, L.; Lopes, G.K.P.; Yokoyama, J.T.C.; Silva, M.C.; Souza, P.S.C.; Ronix, A.; Cazetta, A.L.; Almeida, V.C. Caffeine Adsorption on Activated Biochar Derived from Macrophytes (*Eichornia crassipes*). *J. Mol. Liq.* **2021**, *340*, 117206. [CrossRef]
7. Ziylan-Yavas, A.; Ince, N.H.; Ozon, E.; Arslan, E.; Aviyente, V.; Savun-Hekimoğlu, B.; Erdincler, A. Oxidative Decomposition and Mineralization of Caffeine by Advanced Oxidation Processes: The Effect of Hybridization. *Ultrason. Sonochem.* **2021**, *76*, 105635. [CrossRef]
8. Wang, L.; Zhang, Q.; Chen, B.; Bu, Y.; Chen, Y.; Ma, J.; Rosario-Ortiz, F.L. Photolysis and Photocatalysis of Haloacetic Acids in Water: A Review of Kinetics, Influencing Factors, Products, Pathways, and Mechanisms. *J. Hazard. Mater.* **2020**, *391*, 122143. [CrossRef]
9. Nawaz, T.; Sengupta, S. Contaminants of Emerging Concern: Occurrence, Fate, and Remediation. In *Advances in Water Purification Techniques*; Elsevier: Amsterdam, The Netherlands, 2019; pp. 67–114.
10. Venecia-Nuñez, J.D.; Ramírez-Parra, L.T.; Lara-Ramos, J.A.; Machuca-Martinez, F.; Colina-Márquez, J.Á.; Mueses, M.A. Evaluation of Photocatalysis Based on Ozone/Goethite/Ultraviolet C for Caffeine Degradation. *Chem. Eng. Technol.* **2023**, *46*, 1845–1853. [CrossRef]
11. Tayebee, R.; Esmaeili, E.; Maleki, B.; Khoshniat, A.; Chahkandi, M.; Mollania, N. Photodegradation of Methylene Blue and Some Emerging Pharmaceutical Micropollutants with an Aqueous Suspension of WZnO-NH_2@$H_3PW_{12}O_{40}$ Nanocomposite. *J. Mol. Liq.* **2020**, *317*, 113928. [CrossRef]
12. Zubieta, C.E.; Messina, P.V.; Luengo, C.; Dennehy, M.; Pieroni, O.; Schulz, P.C. Reactive Dyes Remotion by Porous TiO_2-Chitosan Materials. *J. Hazard. Mater.* **2008**, *152*, 765–777. [CrossRef]
13. Simionato, J.I.; Paulino, A.T.; Garcia, J.C.; Nozaki, J. Adsorption of Aluminium from Wastewater by Chitin and Chitosan Produced from Silkworm Chrysalides. *Polym. Int.* **2006**, *55*, 1243–1248. [CrossRef]
14. Saiyad, M.; Shah, N.; Joshipura, M.; Dwivedi, A.; Pillai, S. Chitosan and Its Derivatives in Wastewater Treatment Application. *Mater. Today Proc.* **2024**, *99*, 190–194. [CrossRef]
15. Alshahrani, H.; Abdulhameed, A.S.; Khan, M.K.A.; Al Omari, R.H.; Algburi, S. Functionalization of Chitosan/Alumina Nanoparticles with Carboxylic Groups Using Phthalic Anhydride for Adsorption of Methylene Blue Dye via Response Surface Methodology. *Polym. Bull.* **2025**, *82*, 87–109. [CrossRef]
16. Pavoni, J.M.F.; dos Santos, N.Z.; May, I.C.; Pollo, L.D.; Tessaro, I.C. Impact of Acid Type and Glutaraldehyde Crosslinking in the Physicochemical and Mechanical Properties and Biodegradability of Chitosan Films. *Polym. Bull.* **2021**, *78*, 981–1000. [CrossRef]
17. Mo, Y.; Zhang, F.; Dong, H.; Zhang, X.; Gao, S.; Zhang, S.; Jin, J. Ultrasmall $Cu_3(PO_4)_2$ Nanoparticles Reinforced Hydrogel Membrane for Super-Antifouling Oil/Water Emulsion Separation. *ACS Nano* **2022**, *16*, 20786–20795. [CrossRef]
18. Amiri, S.; Vatanpour, V.; He, T. Antifouling Thin-Film Nanocomposite NF Membrane with Polyvinyl Alcohol-Sodium Alginate-Graphene Oxide Nanocomposite Hydrogel Coated Layer for As(III) Removal. *Chemosphere* **2023**, *322*, 138159. [CrossRef]
19. Rajabi, N.; Masrournia, M.; Abedi, M. Measuring and Pre-Concentration of Lanthanum Using Fe_3O_4@Chitosan Nanocomposite with Solid-Phase Microextraction for ICP-OES Determination. *Arab. J. Sci. Eng.* **2020**, *45*, 121–129. [CrossRef]
20. Yang, J.M.; Su, W.Y. Preparation and Characterization of Chitosan Hydrogel Membrane for the Permeation of 5-Fluorouracil. *Mater. Sci. Eng. C* **2011**, *31*, 1002–1009. [CrossRef]
21. Ahmad, A.L.; Yusuf, N.M.; Ooi, B.S. Preparation and Modification of Poly (Vinyl) Alcohol Membrane: Effect of Crosslinking Time towards Its Morphology. *Desalination* **2012**, *287*, 35–40. [CrossRef]
22. Haripriyan, U.; Gopinath, K.P.; Arun, J. Chitosan Based Nano Adsorbents and Its Types for Heavy Metal Removal: A Mini Review. *Mater. Lett.* **2022**, *312*, 131670. [CrossRef]
23. Matsuyama, H.; Shiraishi, H.; Kitamura, Y. Effect of Membrane Preparation Conditions on Solute Permeability in Chitosan Membrane. *J. Appl. Polym. Sci.* **1999**, *73*, 2715–2725. [CrossRef]
24. Prieto-Rodriguez, L.; Miralles-Cuevas, S.; Oller, I.; Agüera, A.; Puma, G.L.; Malato, S. Treatment of Emerging Contaminants in Wastewater Treatment Plants (WWTP) Effluents by Solar Photocatalysis Using Low TiO_2 Concentrations. *J. Hazard. Mater.* **2012**, *211–212*, 131–137. [CrossRef] [PubMed]
25. Koe, W.S.; Lee, J.W.; Chong, W.C.; Pang, Y.L.; Sim, L.C. An Overview of Photocatalytic Degradation: Photocatalysts, Mechanisms, and Development of Photocatalytic Membrane. *Environ. Sci. Pollut. Res.* **2020**, *27*, 2522–2565. [CrossRef] [PubMed]
26. Maqbool, A. Photocatalytic Degradation Properties. *Charact. Appl. Nanomater.* **2024**, *7*, 5523. [CrossRef]
27. Aoudjit, L.; Zioui, D.; Touahra, F.; Mahidine, S.; Bachari, K. Photocatalytic Degradation of Tartrazine Dyes Using TiO_2–Chitosan Beads under Sun Light Irradiation. *Russ. J. Phys. Chem. A* **2021**, *95*, 1069–1076. [CrossRef]

28. Savun-Hekimoğlu, B.; Eren, Z.; Ince, N.H. Photocatalytic Destruction of Caffeine on Sepiolite-Supported TiO_2 Nanocomposite. *Sustainability* **2020**, *12*, 10314. [CrossRef]
29. Giri, R.R.; Ozaki, H.; Ota, S.; Taniguchi, S.; Takanami, R. Influence of Inorganic Solids on Photocatalytic Oxidation of 2,4-Dichlorophenoxyacetic Acid with UV and TiO_2 Fiber in Aqueous Solution. *Desalination* **2010**, *255*, 9–14. [CrossRef]
30. Marques, R.R.N.; Sampaio, M.J.; Carrapiço, P.M.; Silva, C.G.; Morales-Torres, S.; Dražić, G.; Faria, J.L.; Silva, A.M.T. Photocatalytic Degradation of Caffeine: Developing Solutions for Emerging Pollutants. *Catal. Today* **2013**, *209*, 108–115. [CrossRef]
31. Kanakaraju, D.; Ravichandar, S.; Lim, Y.C. Combined Effects of Adsorption and Photocatalysis by Hybrid TiO_2/ZnO-Calcium Alginate Beads for the Removal of Copper. *J. Environ. Sci.* **2017**, *55*, 214–223. [CrossRef]
32. Paz, M.J.; Vieira, T.; Enzweiler, H.; Paulino, A.T. Chitosan/Wood Sawdust/Magnetite Composite Membranes for the Photodegradation of Agrochemicals in Water. *J. Environ. Chem. Eng.* **2022**, *10*, 106967. [CrossRef]
33. Aparecida Matias, C.; Vilela, P.B.; Becegato, V.A.; Paulino, A.T. Adsorption Kinetic, Isotherm and Thermodynamic of 2,4-Dichlorophenoxyacetic Acid Herbicide in Novel Alternative Natural Adsorbents. *Water Air Soil Pollut.* **2019**, *230*, 276. [CrossRef]
34. Das, R.S.; Kumar, A.; Wankhade, A.V.; Peshwe, D.R. ZrO_2@chitosan Composite for Simultaneous Photodegradation of Three Emerging Contaminants and Antibacterial Application. *Carbohydr. Polym.* **2022**, *278*, 118940. [CrossRef]
35. Zioui, D.; Aoudjit, L.; Touahra, F.; Bachari, K. Preparation and characterization of TiO_2-chitosan composite films and application for tartrazine dye degradation. *Cellul. Chem. Technol.* **2022**, *56*, 1101–1107. [CrossRef]
36. Costa, E.d.S., Jr.; Mansur, H.S. Preparação e Caracterização de Blendas de Quitosana/Poli(Álcool Vinílico) Reticuladas Quimicamente Com Glutaraldeído Para Aplicação Em Engenharia de Tecido. *Química Nova* **2008**, *31*, 1460–1466. [CrossRef]
37. da Cruz, L.F.; Polizeli, A.G.; Enzweiler, H.; Paulino, A.T. Chitosan-Co-GLU/Eucalyptus Residue Composite Membrane for the Stabilization of β-d-Galactosidase in Aqueous Solutions. *Polym. Bull.* **2024**, *81*, 6437–6455. [CrossRef]
38. Vieira, T.; Becegato, V.A.; Paulino, A.T. Equilibrium Isotherms, Kinetics, and Thermodynamics of the Adsorption of 2,4-Dichlorophenoxyacetic Acid to Chitosan-Based Hydrogels. *Water Air Soil Pollut.* **2021**, *232*, 60. [CrossRef]
39. Banafati Zadeh, F.; Zamanian, A. Glutaraldehyde: Introducing Optimum Condition for Cross-Linking the Chitosan/Gelatin Scaffolds for Bone Tissue Engineering. *Int. J. Eng.* **2022**, *35*, 1967–1980. [CrossRef]
40. Wegrzynowska-Drzymalska, K.; Grebicka, P.; Mlynarczyk, D.T.; Chelminiak-Dudkiewicz, D.; Kaczmarek, H.; Goslinski, T.; Ziegler-Borowska, M. Crosslinking of Chitosan with Dialdehyde Chitosan as a New Approach for Biomedical Applications. *Materials* **2020**, *13*, 3413. [CrossRef]
41. Geeta; Shivani; Devi, N.; Shayoraj; Bansal, N.; Sharma, S.; Dubey, S.K.; Kumar, S. Novel Chitosan-Based Smart Bio-Nanocomposite Films Incorporating TiO_2 Nanoparticles for White Bread Preservation. *Int. J. Biol. Macromol.* **2024**, *267*, 131367. [CrossRef]
42. Alzahrani, E.; Ahmed, R.A.; Sattam Alotibi, R. TiO_2NPs Embedded in Chitosan Membrane for Efficient Photodegradation of Various Dyes. *Orient. J. Chem.* **2020**, *36*, 144–160. [CrossRef]
43. Anaya-Esparza, L.M.; Ruvalcaba-Gómez, J.M.; Maytorena-Verdugo, C.I.; González-Silva, N.; Romero-Toledo, R.; Aguilera-Aguirre, S.; Pérez-Larios, A.; Montalvo-González, E. Chitosan-TiO_2: A Versatile Hybrid Composite. *Materials* **2020**, *13*, 811. [CrossRef]
44. Vilela, P.B.; Matias, C.A.; Dalalibera, A.; Becegato, V.A.; Paulino, A.T. Polyacrylic Acid-Based and Chitosan-Based Hydrogels for Adsorption of Cadmium: Equilibrium Isotherm, Kinetic and Thermodynamic Studies. *J. Environ. Chem. Eng.* **2019**, *7*, 103327. [CrossRef]
45. Ali, F.; Khan, S.B.; Kamal, T.; Alamry, K.A.; Asiri, A.M. Chitosan-Titanium Oxide Fibers Supported Zero-Valent Nanoparticles: Highly Efficient and Easily Retrievable Catalyst for the Removal of Organic Pollutants. *Sci. Rep.* **2018**, *8*, 6260. [CrossRef] [PubMed]
46. Wongniramaikul, W.; Kleangklao, B.; Sadegh, F.; Sadegh, N.; Choodum, A. Highly Efficient Phosphate Adsorption Using Calcium Silicate Hydrate-Embedded Calcium Crosslinked Polyvinyl Alcohol Thin Film. *Environ. Res.* **2024**, *263*, 120229. [CrossRef] [PubMed]
47. Liu, Q.; Hu, P.; Wang, J.; Zhang, L.; Huang, R. Phosphate Adsorption from Aqueous Solutions by Zirconium (IV) Loaded Cross-Linked Chitosan Particles. *J. Taiwan. Inst. Chem. Eng.* **2016**, *59*, 311–319. [CrossRef]
48. Isidoro Ribeiro, N.; Barreto Pessanha, O.; Luiza Gomes Soares Pessanha, M.; Guimarães, D. Efficient Phosphate Adsorption by a Composite Composed of $Mg_6Al_2(CO_3)(OH)_{16}{\cdot}4H_2O$ LDH and Chitosan: Kinetic, Thermodynamic, Desorption, and Characterization Studies. *Sep. Purif. Technol.* **2023**, *307*, 122717. [CrossRef]
49. Banu, H.T.; Meeenakshi, S. Effective Removal of Phosphate from Aqueous Solution by Lanthanum Loaded Bio-Polymeric Composite. *Mater. Today Proc.* **2018**, *5*, 16165–16171. [CrossRef]
50. Liu, X.; Zhang, L. Removal of Phosphate Anions Using the Modified Chitosan Beads: Adsorption Kinetic, Isotherm and Mechanism Studies. *Powder Technol.* **2015**, *277*, 112–119. [CrossRef]
51. Eltaweil, A.S.; Abd El-Monaem, E.M.; Elshishini, H.M.; El-Aqapa, H.G.; Hosny, M.; Abdelfatah, A.M.; Ahmed, M.S.; Hammad, E.N.; El-Subruiti, G.M.; Fawzy, M.; et al. Recent Developments in Alginate-Based Adsorbents for Removing Phosphate Ions from Wastewater: A Review. *RSC Adv.* **2022**, *12*, 8228–8248. [CrossRef]

52. Stefanowska, K.; Woźniak, M.; Sip, A.; Mrówczyńska, L.; Majka, J.; Kozak, W.; Dobrucka, R.; Ratajczak, I. Characteristics of Chitosan Films with the Bioactive Substances—Caffeine and Propolis. *J. Funct. Biomater.* **2023**, *14*, 358. [CrossRef]
53. Lewandowska, K. Miscibility and Thermal Stability of Poly(Vinyl Alcohol)/Chitosan Mixtures. *Thermochim. Acta* **2009**, *493*, 42–48. [CrossRef]
54. Paulino, A.T.; Pereira, A.G.B.; Fajardo, A.R.; Erickson, K.; Kipper, M.J.; Muniz, E.C.; Belfiore, L.A.; Tambourgi, E.B. Natural Polymer-Based Magnetic Hydrogels: Potential Vectors for Remote-Controlled Drug Release. *Carbohydr. Polym.* **2012**, *90*, 1216–1225. [CrossRef]
55. Guinesi, L.S.; Cavalheiro, É.T.G. The Use of DSC Curves to Determine the Acetylation Degree of Chitin/Chitosan Samples. *Thermochim. Acta* **2006**, *444*, 128–133. [CrossRef]
56. Zong, Z.; Kimura, Y.; Takahashi, M.; Yamane, H. Characterization of Chemical and Solid State Structures of Acylated Chitosans. *Polymer* **2000**, *41*, 899–906. [CrossRef]
57. Farzana, M.H.; Meenakshi, S. Synergistic Effect of Chitosan and Titanium Dioxide on the Removal of Toxic Dyes by the Photodegradation Technique. *Ind. Eng. Chem. Res.* **2014**, *53*, 55–63. [CrossRef]
58. Lin, B.; Luo, Y.; Teng, Z.; Zhang, B.; Zhou, B.; Wang, Q. Development of Silver/Titanium Dioxide/Chitosan Adipate Nanocomposite as an Antibacterial Coating for Fruit Storage. *LWT—Food Sci. Technol.* **2015**, *63*, 1206–1213. [CrossRef]
59. Fahmy, T.; Sarhan, A. Characterization and Molecular Dynamic Studies of Chitosan–Iron Complexes. *Bull. Mater. Sci.* **2021**, *44*, 142. [CrossRef]
60. Anirudhan, T.S.; Nair, S.S.; Nair, A.S. Fabrication of a Bioadhesive Transdermal Device from Chitosan and Hyaluronic Acid for the Controlled Release of Lidocaine. *Carbohydr. Polym.* **2016**, *152*, 687–698. [CrossRef]
61. Paulino, A.T.; Guilherme, M.R.; Mattoso, L.H.C.; Tambourgi, E.B. Smart Hydrogels Based on Modified Gum Arabic as a Potential Device for Magnetic Biomaterial. *Macromol. Chem. Phys.* **2010**, *211*, 1196–1205. [CrossRef]
62. Barleany, D.R.; Jayanudin, J.; Nasihin, N.; Widiawati, M.; Yulvianti, M.; Sari, D.K.; Gunawan, A. Hydrogel Preparation from Shrimp Shell-Based Chitosan: The Degree of Crosslinking and Swelling Study. *ASEAN J. Chem. Eng.* **2023**, *23*, 28. [CrossRef]
63. Ostrowska-Czubenko, J.; Gierszewska, M.; Pieróg, M. PH-Responsive Hydrogel Membranes Based on Modified Chitosan: Water Transport and Kinetics of Swelling. *J. Polym. Res.* **2015**, *22*, 153. [CrossRef]
64. Jiang, X.; Li, C.; Han, Q. Modulation of Swelling of PVA Hydrogel by Polymer and Crosslinking Agent Concentration. *Polym. Bull.* **2023**, *80*, 1303–1320. [CrossRef]
65. Rani, C.N. Feasibility Study on the Utilization of Low-Cost Sawdust for Adsorption of Caffeine: Equilibrium, Optimization, and Response Surface Modeling. *Desalination Water Treat.* **2022**, *276*, 271–281. [CrossRef]
66. Hu, P.; Liu, Q.; Wang, J.; Huang, R. Phosphate Removal by Ce(III)-impregnated Crosslinked Chitosan Complex from Aqueous Solutions. *Polym. Eng. Sci.* **2017**, *57*, 44–51. [CrossRef]
67. Miotto, A.C.; Orchulhak, A.P.; Enzweiler, H.; Paulino, A.T.; Visioli, L.J. Caffeine Removal from Water Using Rice Husk Residue Biochar: Characterization, Kinetics and Sorption Isotherms. *Int. J. Environ. Sci. Technol.* **2025**, *22*, 7197–7210. [CrossRef]
68. Castañeda, C.; Martínez, J.J.; Santos, L.; Rojas, H.; Osman, S.M.; Gómez, R.; Luque, R. Caffeine Photocatalytic Degradation Using Composites of NiO/TiO_2–F and CuO/TiO_2–F under UV Irradiation. *Chemosphere* **2022**, *288*, 132506. [CrossRef]
69. Shu, Z.; Bolton, J.R.; Belosevic, M.; Gamal El Din, M. Photodegradation of Emerging Micropollutants Using the Medium-Pressure UV/H_2O_2 Advanced Oxidation Process. *Water Res.* **2013**, *47*, 2881–2889. [CrossRef]
70. Lakshmipathy, K.; Sindhu, S.; Singh, A.; Chikkaballapur Krishnappa, S.; Duggonahally Veeresh, C. A Review on Pesticides Degradation by Using Ultraviolet Light Treatment in Agricultural Commodities. *eFood* **2024**, *5*, e129. [CrossRef]
71. Ferens, T.F.; Visioli, L.J.; Paulino, A.T.; Enzweiler, H. Photodegradation of Ibuprofen by Pd-TiO_2/ZSM-5 Catalyst. *Int. J. Environ. Sci. Technol.* **2025**, *22*, 6759–6768. [CrossRef]
72. Minyeong Hong, A.Z. Insights into the Eco-Friendly Adsorption of Caffeine from Contaminated Solutions by Using Hydrogel Beads. *J. Environ. Anal. Chem.* **2015**, *2*, 1–5. [CrossRef]
73. Copello, G.J.; Mebert, A.M.; Raineri, M.; Pesenti, M.P.; Diaz, L.E. Removal of Dyes from Water Using Chitosan Hydrogel/SiO_2 and Chitin Hydrogel/SiO_2 Hybrid Materials Obtained by the Sol–Gel Method. *J. Hazard. Mater.* **2011**, *186*, 932–939. [CrossRef] [PubMed]
74. Young, T.A.; Heidler, J.; Matos-Pérez, C.R.; Sapkota, A.; Toler, T.; Gibson, K.E.; Schwab, K.J.; Halden, R.U. Ab Initio and in Situ Comparison of Caffeine, Triclosan, and Triclocarban as Indicators of Sewage-Derived Microbes in Surface Waters. *Environ. Sci. Technol.* **2008**, *42*, 3335–3340. [CrossRef]
75. Sanford, S.; Singh, K.S.; Chaini, S.; LeClair, G. Study of Natural Adsorbent Chitosan and Derivatives for the Removal of Caffeine from Water. *Water Qual. Res. J.* **2012**, *47*, 80–90. [CrossRef]
76. Sowmya, A.; Meenakshi, S. An Efficient and Regenerable Quaternary Amine Modified Chitosan Beads for the Removal of Nitrate and Phosphate Anions. *J. Environ. Chem. Eng.* **2013**, *1*, 906–915. [CrossRef]
77. Do, T.M.P.; Nguyen, X.L. Adsorption Capacity of Chitosan Hydrogel Beads Fabricated from Penaeus Monodon Shrimp Shell Waste for Safranin o Dye. *Hue Univ. J. Sci. Nat. Sci.* **2023**, *132*, 23–32. [CrossRef]

78. Elhalil, A.; Elmoubarki, R.; Farnane, M.; Machrouhi, A.; Sadiq, M.; Mahjoubi, F.Z.; Qourzal, S.; Barka, N. Photocatalytic Degradation of Caffeine as a Model Pharmaceutical Pollutant on Mg Doped ZnO-Al2O3 Heterostructure. *Environ. Nanotechnol. Monit. Manag.* **2018**, *10*, 63–72. [CrossRef]
79. Kumeda, T.; Sakaushi, K. Joint Kinetic/In Situ Spectrometric Investigation of the Multielectron/Multiproton-Transfer-Based Adsorption Electrode Process of Phosphate Anions on the Ir(111) Surface across a Comprehensive PH Range. *J. Phys. Chem. C* **2023**, *127*, 10341–10354. [CrossRef]
80. Tang, X.; Zhao, S.; Xie, H.; Zhang, Y. Utilization and Value-Adding of Waste: Fabrication of Porous Material from Chitosan for Phosphate Capture and Energy Storage. *Int. J. Biol. Macromol.* **2024**, *268*, 131944. [CrossRef]
81. G., G.; D'Souza, J.Q.; Sundaram, N.G. UV Induced Photocatalytic Degradation of Caffeine Using TiO_2–H-Beta Zeolite Composite. *Minerals* **2023**, *13*, 465. [CrossRef]
82. Liao, W.; Zhao, M.; Rong, H.; Jiang, P.; Liao, Q.; Zhang, C.; Chen, Y. Photocatalyst Immobilized by Hydrogel, Efficient Degradation and Self Regeneration: A Review. *Mater. Sci. Semicond. Process.* **2022**, *150*, 106929. [CrossRef]
83. Nirmala Rani, C. Photocatalytic Degradation of Caffeine in a Slurry Reactor with Intermittent UV Irradiation: Optimization and Response Surface Modelling. *Water Pract. Technol.* **2022**, *17*, 517–528. [CrossRef]
84. Zhao, D.; Chen, C.; Wang, Y.; Ji, H.; Ma, W.; Zang, L.; Zhao, J. Surface Modification of TiO_2 by Phosphate: Effect on Photocatalytic Activity and Mechanism Implication. *J. Phys. Chem. C* **2008**, *112*, 5993–6001. [CrossRef]
85. Muangmora, R.; Kemacheevakul, P.; Punyapalakul, P.; Chuangchote, S. Enhanced Photocatalytic Degradation of Caffeine Using Titanium Dioxide Photocatalyst Immobilized on Circular Glass Sheets under Ultraviolet C Irradiation. *Catalysts* **2020**, *10*, 964. [CrossRef]
86. Rahman, T.U.; Roy, H.; Shoronika, A.Z.; Fariha, A.; Hasan, M.; Islam, M.S.; Marwani, H.M.; Islam, A.; Hasan, M.M.; Alsukaibi, A.K.D.; et al. Sustainable Toxic Dye Removal and Degradation from Wastewater Using Novel Chitosan-Modified TiO_2 and ZnO Nanocomposites. *J. Mol. Liq.* **2023**, *388*, 122764. [CrossRef]
87. Lado Ribeiro, A.R.; Moreira, N.F.F.; Li Puma, G.; Silva, A.M.T. Impact of Water Matrix on the Removal of Micropollutants by Advanced Oxidation Technologies. *Chem. Eng. J.* **2019**, *363*, 155–173. [CrossRef]
88. Heydari Orojlou, S.; Rastegarzadeh, S.; Zargar, B. Experimental and Modeling Analyses of COD Removal from Industrial Wastewater Using the TiO_2–Chitosan Nanocomposites. *Sci. Rep.* **2022**, *12*, 11088. [CrossRef]
89. Almeida, L.N.B.; Pietrobelli, J.M.T.A.; Lenzi, G.G.; Santos, O.A.A. Degradation of Caffeine by Heterogeneous Photocatalysis Using ZnO with Fe and Ag. *Braz. Arch. Biol. Technol.* **2020**, *63*, 1–9. [CrossRef]
90. Gonçalves, M.; Guerreiro, M.C.; Oliveira, L.C.A.; Rocha, C.L. da Materiais à Base de Óxido de Ferro Para Oxidação de Compostos Presentes No Efluente Da Despolpa Do Café. *Química Nova* **2008**, *31*, 1636–1640. [CrossRef]
91. Reinehr, I.L.; Capra, D.F.; Kempka, A.P.; Visioli, L.J.; Paulino, A.T.; Enzweiler, H. Innovative Chitosan/TiO_2 Composite Membrane for the Sustainable Photocatalytic Purification of Water Contaminated with Emerging Micropollutants. *Polym. Bull.* 2025, *in press*. [CrossRef]

Disclaimer/Publisher's Note: The statements, opinions and data contained in all publications are solely those of the individual author(s) and contributor(s) and not of MDPI and/or the editor(s). MDPI and/or the editor(s) disclaim responsibility for any injury to people or property resulting from any ideas, methods, instructions or products referred to in the content.